Supporting Information for

Seeded Growth: A Potentially General Synthesis of Monodisperse Metallic Nanoparticles

Heng Yu, Patrick C. Gibbons, and William E. Buhro*

Departments of Chemistry and Physics,
Washington University, St. Louis, Missouri, 63130-4899

Table of Contents:

Experimental Procedures

General. All ambient-pressure procedures were carried out under dry N_2 using standard inert-atmosphere techniques. The nanoparticle products were generally stored and handled under inert atmospheres. However, air exposure for up to 1 h, while preparing samples for TEM analysis or during collection of XRD data, did not result in observable decomposition or other obvious changes in the samples.

Estimation of nanoparticle yields. The precipitated products contained both the polymer added and the metallic nanoparticles formed. A theoretical mass yield $m_{theor} = (m_{metal} + m_{polymer})$ was therefore based on the total amounts of metallic precursor and polymer employed. Calculation of yield from this m_{theor} and the measured product masses m_{obs} assumed retention of the theoretical metallic mass fraction $[m_{metal}/(m_{metal} + m_{polymer})]$ in the precipitated product. The latter assumption is most valid for cases of high metallic mass fraction, where small deviations from the theoretical values would generate only small errors in the nanoparticle-yield calculations. The assumption is invalid for cases of low metallic mass fraction, where small deviations would generate large errors in the yield calculations. Thus, we do not estimate a yield for Bi nanoparticles (for which the theoretical metallic mass fraction was only 0.06).

Materials. The precursors $Au_{101}(PPh_3)_{21}Cl_5$,[22] $Bi[N(SiMe_3)_2]_3$,[23] $Sn(NMe_2)_2$,[24] and $In(C_5H_5)$[25] were prepared according to literature methods. 1-Vinyl-2-pyrrolidinone and styrene were obtained from Aldrich and vacuum distilled before use. Methanol and isopropanol were distilled from Mg/I_2. 2,2'-azobisisobutyronitrile (AIBN) was obtained from Aldrich and recrystallized from methanol. Poly(vinylpyrrolidinone) (PVP, M_n 10,000 g/mol), $Na[Na(SiMe_3)_2]$, and $Li[NMe_2]$ were used as received from Aldrich. Anhydrous THF was obtained from Aldrich packaged under N_2 in Sure/Seal^{TM} bottles. The solvent 1,3-

diisopropylbenzene was shaken with concentrated sulfuric acid to remove thiophene, washed with water, and distilled over Na. Benzene was distilled from sodium benzophenone ketyl. Pentane was used as received from Aldrich.

Preparation of poly(styrene$_{0.86}$-*co*-vinylpyrrolidinone$_{0.14}$) (PS$_{0.86}$-*co*-PVP$_{0.14}$). Styrene (170 g, 1.63 mol) and vinylpyrrolidinone (28.7 g, 0.258 mol) were combined in benzene (200 mL). AIBN (2.5 g, 0.152 mol) was added and the stirring reaction mixture was heated to 80 °C for 5 h. Methanol (100 mL) was then added to terminate the reaction. The product polymer was purified by precipitation with pentane (2 L), and the resulting white crystalline solid was dried in vaccum at 100 °C for 3 hrs, yielding 90.0 g (45 %). The molecular weight was determined by gel-permeation chromatography: M_n, 14,013 ± 283 g/mol; M_w, 23,433 ± 134 g/mol; M_z, 39,813 ± 300 g/mol.

Preparation of Stock Solution A, containing Au$_{101}$(PPh$_3$)$_{21}$Cl$_5$. A stock solution of Au seeds was prepared by dissolving $Au_{101}(PPh_3)_{21}Cl_5$ (0.066 g, 2.6×10^{-6} mol, M = 25,578 g/mol) in THF (48 g), yielding a solution having a molality of $m = 5.4 \times 10^{-5}$ mol/kg.

Preparation of Stock Solution B, for use in Bi-nanoparticle synthesis. PS$_{0.86}$-*co*-PVP$_{0.14}$ (8 g) was dissolved in 1,3-diisopropylbenzene (393 g), and Na[Na(SiMe$_3$)$_2$] (0.180 g) was added as a drying agent to scavenge adventitious H_2O.

Preparation of Stock Solution C, for use in Sn-nanoparticle synthesis. PS$_{0.86}$-*co*-PVP$_{0.14}$ (18 g) was dissolved in 1,3-diisopropylbenzene (700 g), and Li[NMe$_2$] (0.120 g) was added as a drying agent to scavenge adventitious H_2O.

Preparation of Stock Solution D, for use in In-nanoparticle synthesis. PVP (0.440 g) was dissolved in THF (95 g), and activated molecular sieves were added as a drying agent to scavenge adventitious H_2O.

Preparation of 12.4-nm Bi nanoparticles (sample Bi/1). Aliquots of stock solutions A (0.100 g) and B (18 g) were combined with $Bi[N(SiMe_3)_2]_3$ (0.056 g, 0.081 mmol) to generate a pale-yellow solution. The reaction vessel was then immersed in an oil bath that had been preheated to 150 ^oC, and the solution color began to darken towards brown immediately. Within 20 – 30 min the solution color had become black, and continued to deepen with subsequent heating. The reaction mixture was heated for a total of 8 h at 150 ^oC, yielding a deep black dispersion of Bi nanoparticles, which contained a very small amount of a black precipitate. When protected from atmospheric exposure, such dispersions were stable for at least several weeks.

The Bi nanoparticles were precipitated as black powders by addition of isopropanol. Initially, the black powders could be re-dispersed in solvents such as benzene, toluene, or THF. However, the nanoparticles became progressively less re-dispersible upon storage in solid form, over time-scales of approximately a week.

Bi nanoparticles exhibiting other mean sizes were prepared similarly, using the reagent quantities and conditions recorded in Table 2.

Preparation of 25.4-nm Sn nanoparticles (sample Sn/1). Aliquots of stock solutions A (0.110 g) and C (10 g) were combined with $Sn(NMe_2)_2$ (0.110 g, 0.531 mmol) to generate a pale-yellow solution. The reaction vessel was then immersed in an oil bath that had been preheated to 140 ^oC, and the solution color began to darken towards brown within 10 min. Within 20 – 30 min the solution color had become black, and continued to deepen with subsequent heating. The reaction mixture was heated for a total of 3 h at 140 ^oC, yielding a deep black dispersion of Sn nanoparticles, which contained a very small amount of a black precipitate. When protected from atmospheric exposure, such dispersions were stable for at least several weeks.

The Sn nanoparticles were precipitated as black powders by addition of isopropanol (90 mg, 29%). Initially, the black powders could be re-dispersed in solvents such as benzene, toluene, or THF. However, the nanoparticles became progressively less re-dispersible upon storage in solid form, over time-scales of approximately a week.

Sn nanoparticles exhibiting other mean sizes were prepared similarly, using the reagent quantities and conditions recorded in Table 2.

Preparation of 9.1-nm In nanoparticles (sample In/2). Aliquots of stock solutions A (0.500 g) and D (7.0 g) were combined with $In(C_5H_5)$ (0.032 g, 0.18 mmol) to generate a colorless solution. Methanol (0.140 g, 4.37 mmol) was added to the stirring solution at room temperature, and the solution color began to darken after an induction period of 1 – 2 min (in contrast, the induction period was 15 min for sample In/1). Within 15 min the solution color had become deep black. Such deep black dispersions of In nanoparticles, which contained very small amounts of black precipitates, were stable for at least several weeks at room temperature when protected from the atmosphere.

In nanoparticles exhibiting other mean sizes were prepared similarly, using the reagent quantities and conditions recorded in Table 2.

The In nanoparticles were precipitated as black powders by addition of pentane (13 mg, 29%). The black powders could be re-dispersed in solvents such as methanol or THF. The larger-sized In nanoparticles became progressively less re-dispersible upon storage in solid form, over time-scales of approximately a week. The smaller-sized In nanoparticles appeared to retain good re-dispersibility upon storage.

Particle-size Analysis by TEM. Samples were prepared by pipetting a few drops of the nanoparticle dispersions onto holey-carbon-coated Cu TEM grids in an N_2-filled glove box, and

allowing the solvents to evaporate. A JEOL 2000 FX instrument operating at 200 kV was used to collect normal bright-field images.

Several images were recorded on film for each sample. The film was developed and printed; the prints and/or negatives were scanned, and each image was plotted on an 8.5 inch × 11 inch scale. The particle sizes from these enlarged images were measured by hand, in some cases using scans of negatives, and in other cases scans of photographic prints. The images used for particle measurement were initially obtained in the TEM at magnifications of either 250K× or 500K×. Representative images used in the analysis of each sample are given in Figures 2 – 10. Uneven backgrounds in the images precluded use of a standard image-analysis software package for particle-size analysis.

The particle sizes manually extracted from the multiple images for an individual sample were entered into a spreadsheet program for statistical determination of mean particle size and the standard deviation. These data and the spreadsheet program were used to construct the particle-size histograms in Figures 11 – 19. Generally, about 200 particles were measured and used in the statistical analyses for each sample. However, in one case the available images contained a total of only 66 measurable nanoparticles, and in two other cases only about 100 particles were measured. The exact number of nanoparticles measured in the statistical analysis of each sample is recorded in Table 2.

Table 2. Quantities and conditions used for preparation of metallic nanoparticles.

Metal/trial	Precursor (amount, mg)	Amount of stock-solution A used, mg	Other stock solution used (amount, g)	Reaction temperature, ^{o}C (reaction time, h)	Nanoparticle mean size,[a] nm (nanoparticles measured)	Amount of methanol used, mg
Bi/1	$Bi[N(SiMe_3)_2]_3$ (56)	100	B (18)	150 (8)	12.4 ± 0.9 (190)	–
Bi/2	$Bi[N(SiMe_3)_2]_3$ (56)	370	B (18)	150 (8)	9.3 ± 0.7 (218)	–
Bi/3	$Bi[N(SiMe_3)_2]_3$ (25)	220	B (10)	150 (8)	8.6 ± 0.5 (66)	–
Sn/1	$Sn(NMe_2)_2$ (110)	110	C (10)	140 (3)	25.4 ± 1.8 (154)	–
Sn/2	$Sn(NMe_2)_2$ (130)	205	C (10.0)	140 (3)	17.3 ± 1.2 (94)	–
Sn/3	$Sn(NMe_2)_2$ (30)	160	C (5.0)	140 (3)	10.5 ± 1.4 (171)	–
In/1	$In(C_5H_5)$ (36)	16	D (4.0)	RT	15.7 ± 1.5 (244)	25
In/2	$In(C_5H_5)$ (35)	280	D (7.0)	RT	9.1 ± 0.9 (259)	220
In/3	$In(C_5H_5)$ (32)	500	D (7.0)	RT	7.1 ± 0.5 (116)	140

[a]The nanoparticle mean size was determined by TEM analysis as described on p. 6. The value following the "±" symbol is equal to 1 standard deviation as determined by statistical analysis from the particle-size distribution.

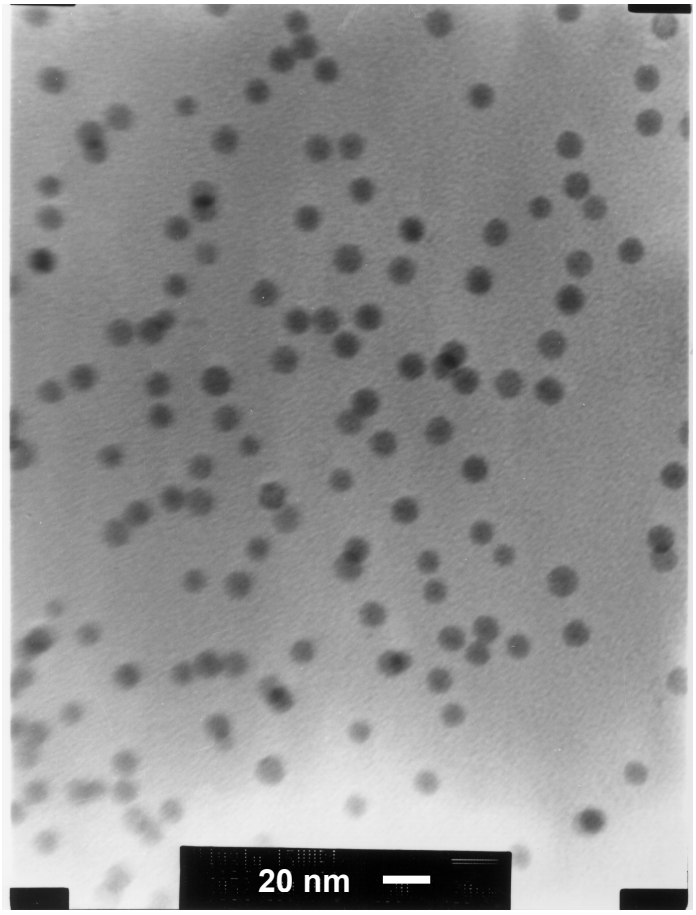

Figure 2. Representative TEM image used for particle-size analysis of sample Bi/1 (mean diameter 12.4 ± 0.9 nm). This image was scaled to fill an 8.5×11 inch^2 sheet for the analysis (manual measurement of particle diameters).

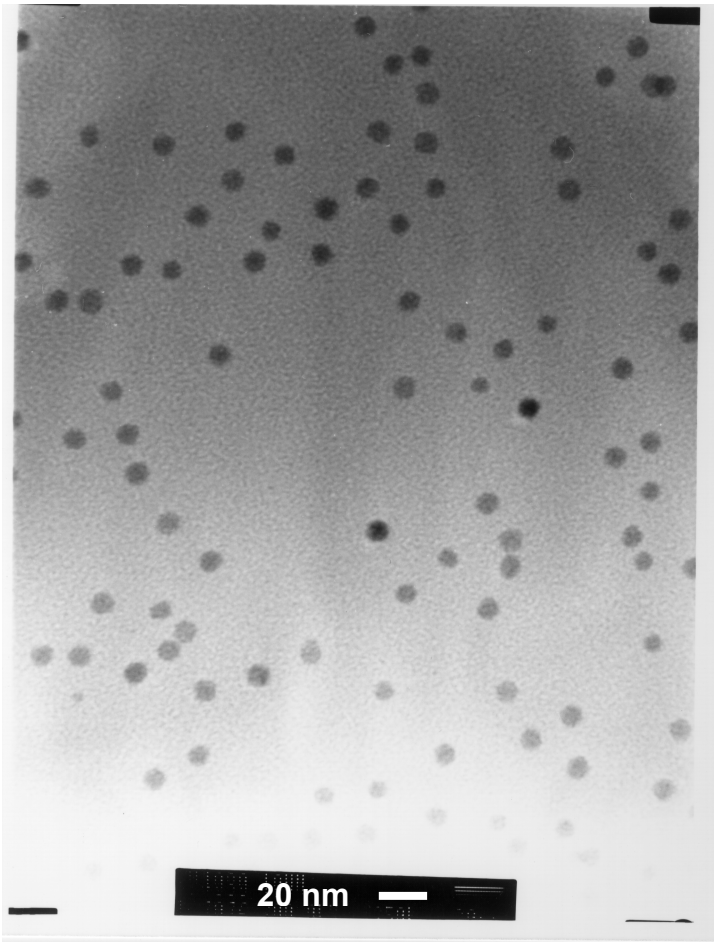

Figure 3. Representative TEM image used for particle-size analysis of sample Bi/2 (mean diameter 9.3 ± 0.7 nm). This image was scaled to fill an 8.5 × 11 inch^2 sheet for the analysis (manual measurement of particle diameters).

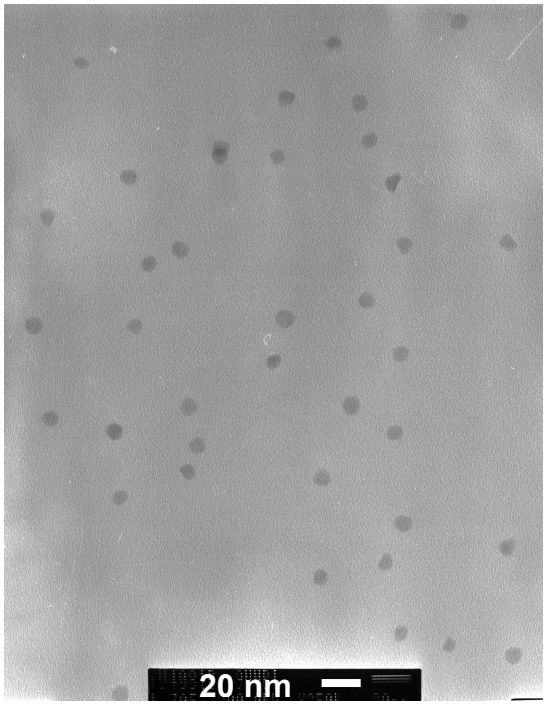

Figure 4. Representative TEM image used for particle-size analysis of sample Bi/3 (mean diameter 8.6 ± 0.5 nm). This image was scaled to fill an 8.5×11 inch^2 sheet for the analysis (manual measurement of particle diameters).

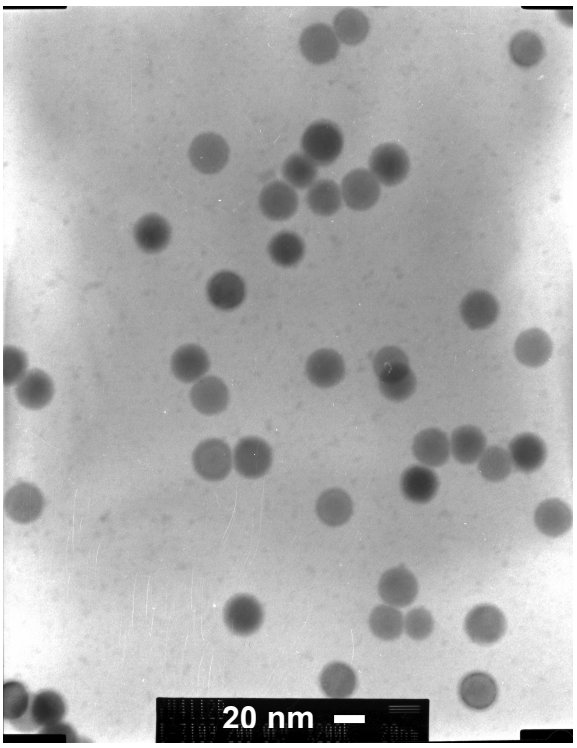

Figure 5. Representative TEM image used for particle-size analysis of sample Sn/1 (mean diameter 25.4 ± 1.8 nm). This image was scaled to fill an 8.5 × 11 inch^2 sheet for the analysis (manual measurement of particle diameters).

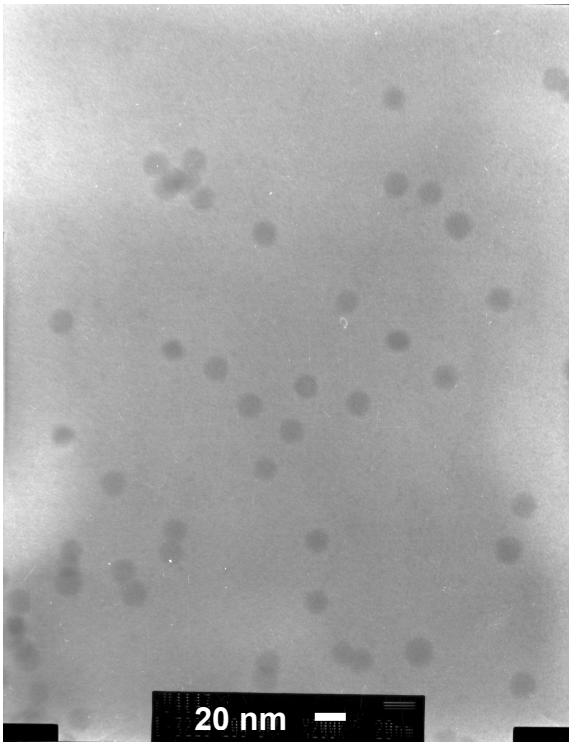

Figure 6. Representative TEM image used for particle-size analysis of sample Sn/2 (mean diameter 17.3 ± 1.2 nm). This image was scaled to fill an 8.5 × 11 inch^2 sheet for the analysis (manual measurement of particle diameters).

.

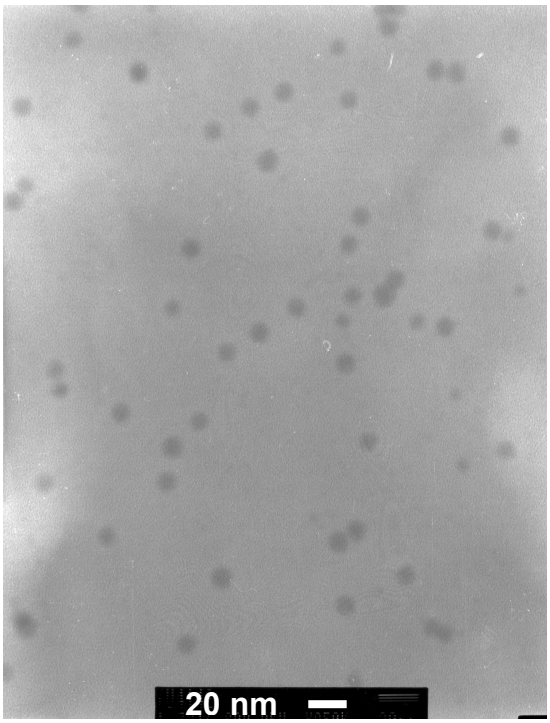

Figure 7. Representative TEM image used for particle-size analysis of sample Sn/3 (mean diameter 10.5 ± 1.4 nm). This image was scaled to fill an 8.5×11 inch^2 sheet for the analysis (manual measurement of particle diameters).

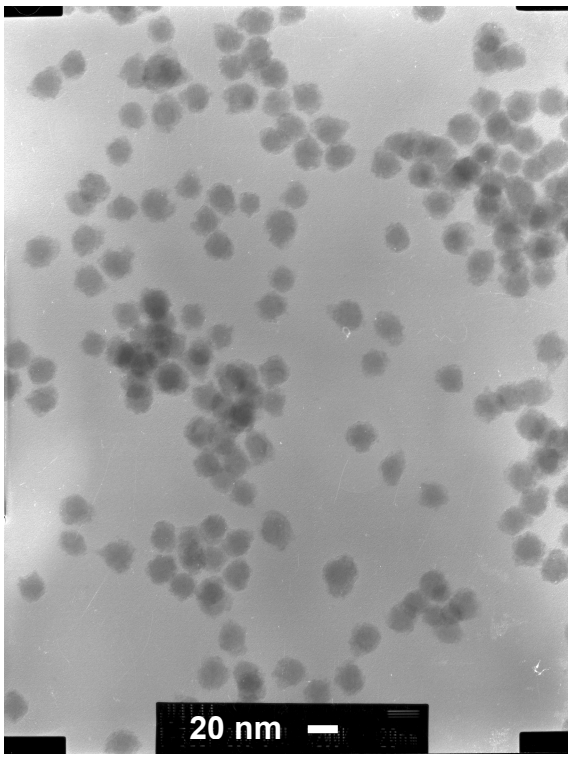

Figure 8. Representative TEM image used for particle-size analysis of sample In/1 (mean diameter 15.7 ± 1.5 nm). This image was scaled to fill an 8.5 × 11 inch^2 sheet for the analysis (manual measurement of particle diameters).

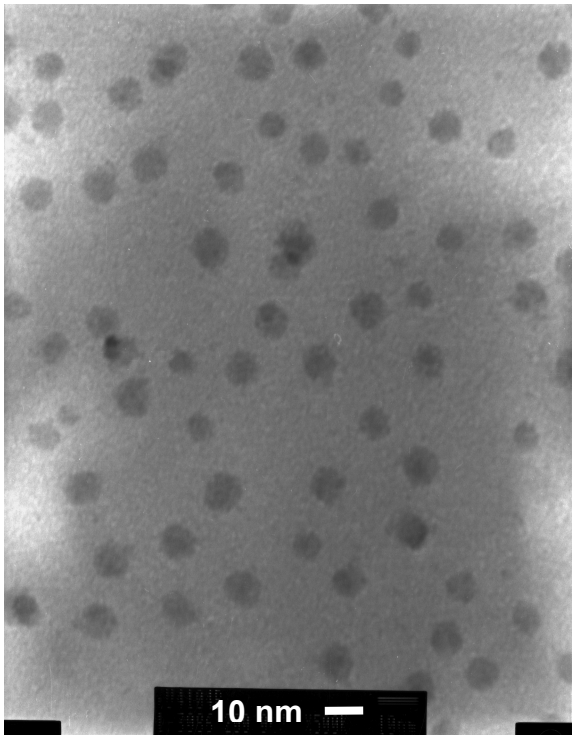

Figure 9. Representative TEM image used for particle-size analysis of sample In/2 (mean diameter 9.1 ± 0.9 nm). This image was scaled to fill an 8.5 × 11 inch^2 sheet for the analysis (manual measurement of particle diameters).

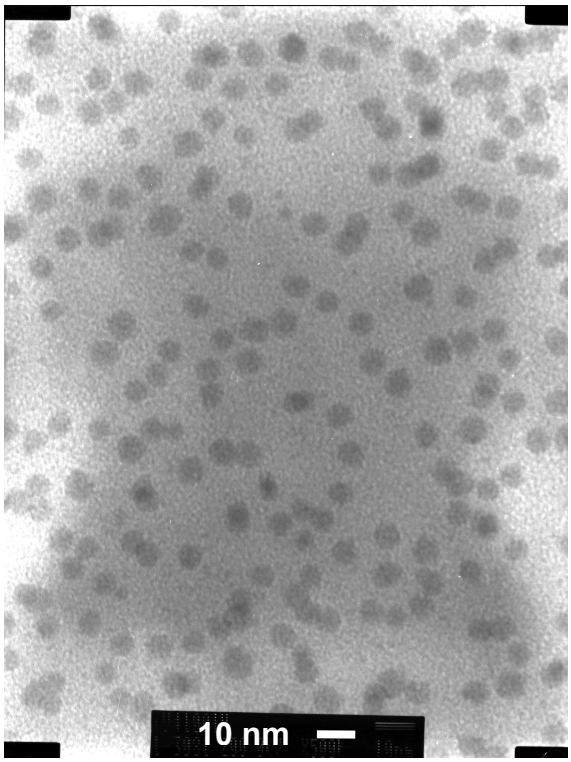

Figure 10. Representative TEM image used for particle-size analysis of sample In/3 (mean diameter 7.1 ± 0.5 nm). This image was scaled to fill an 8.5 × 11 inch^2 sheet for the analysis (manual measurement of particle diameters).

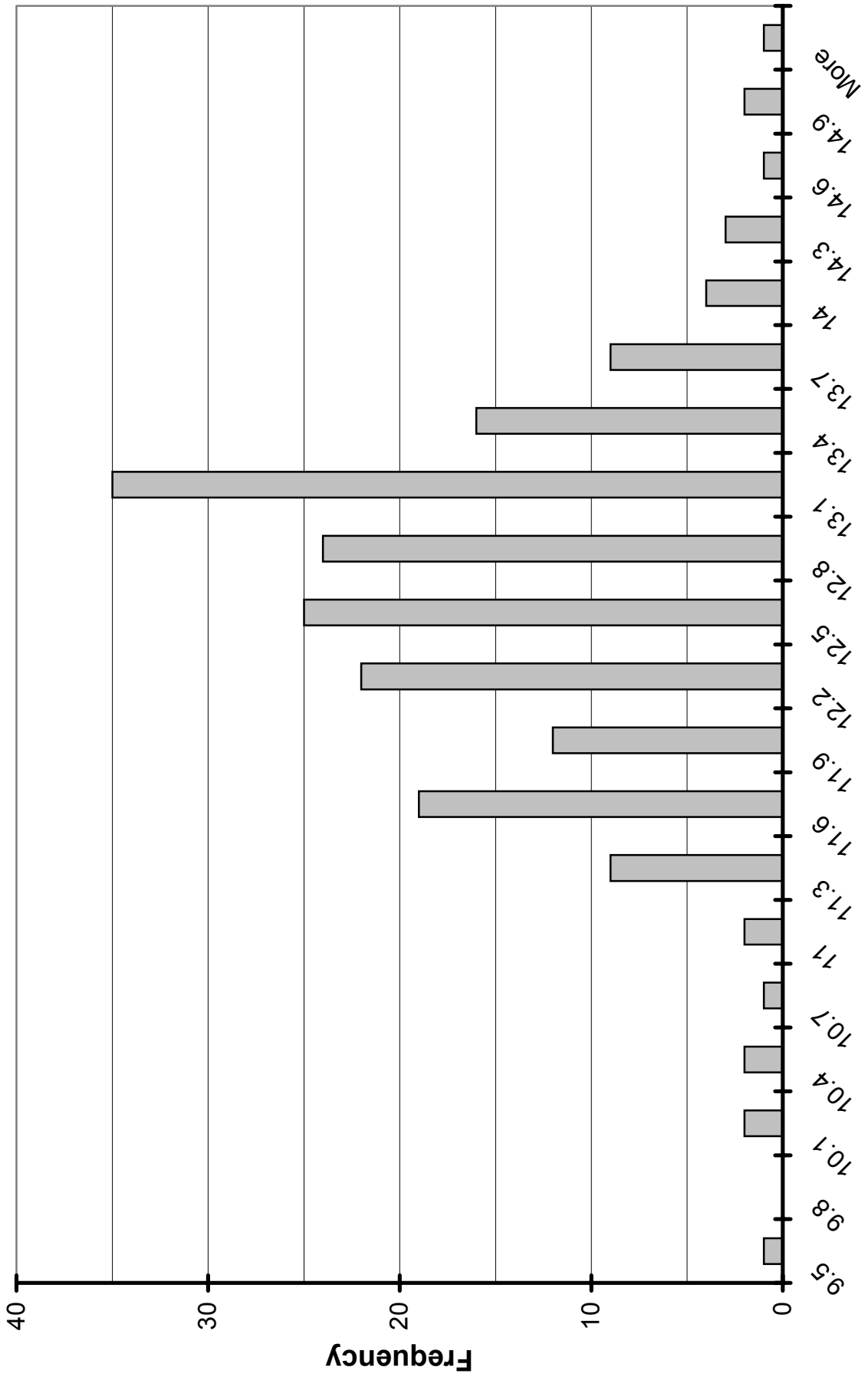

Figure 11. Particle-size histogram for sample Bi/1 (mean diameter 12.4 ± 0.9 nm)

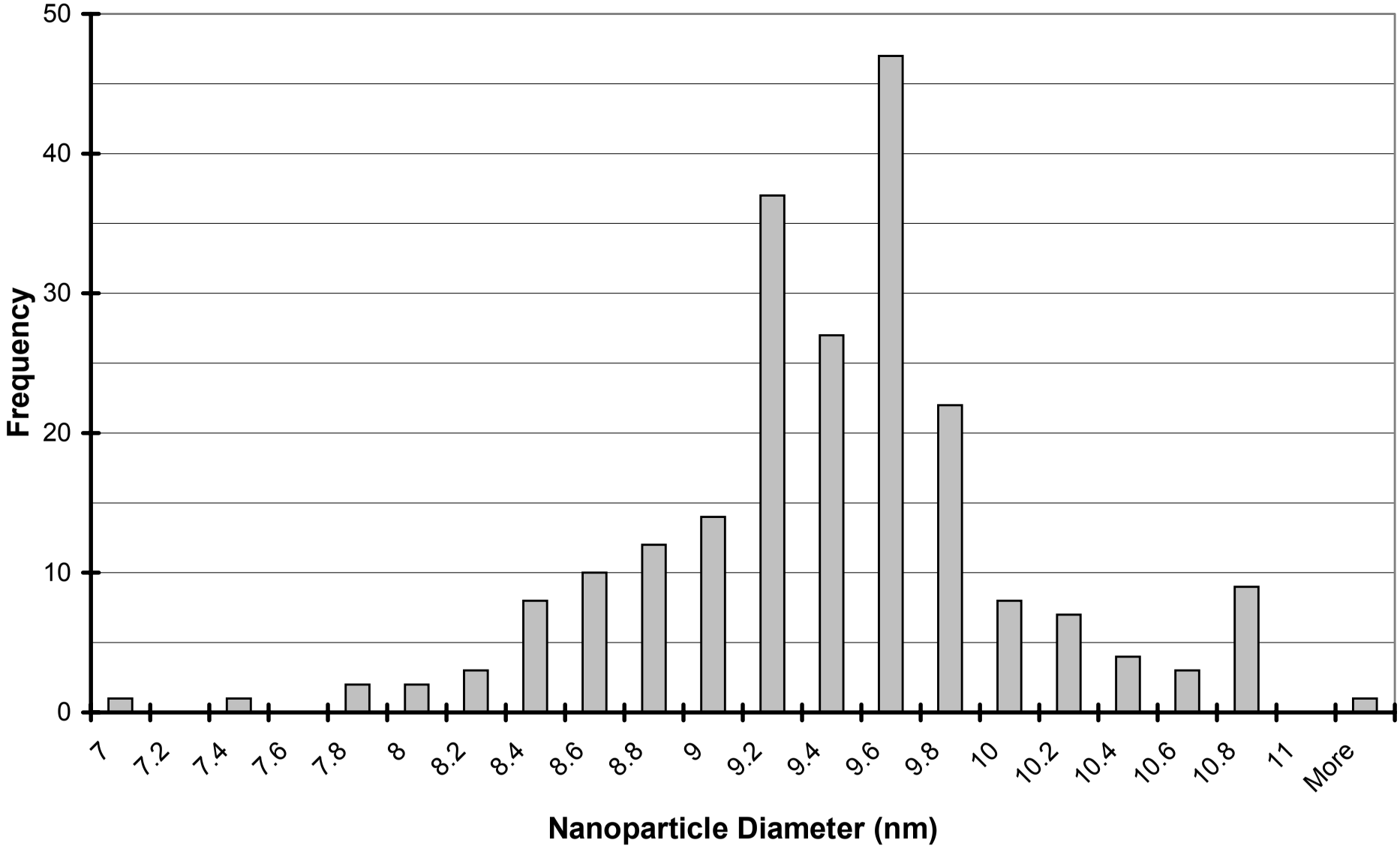

Figure 12. Particle-size histogram for sample Bi/2 (mean diameter 9.3 ± 0.7 nm)

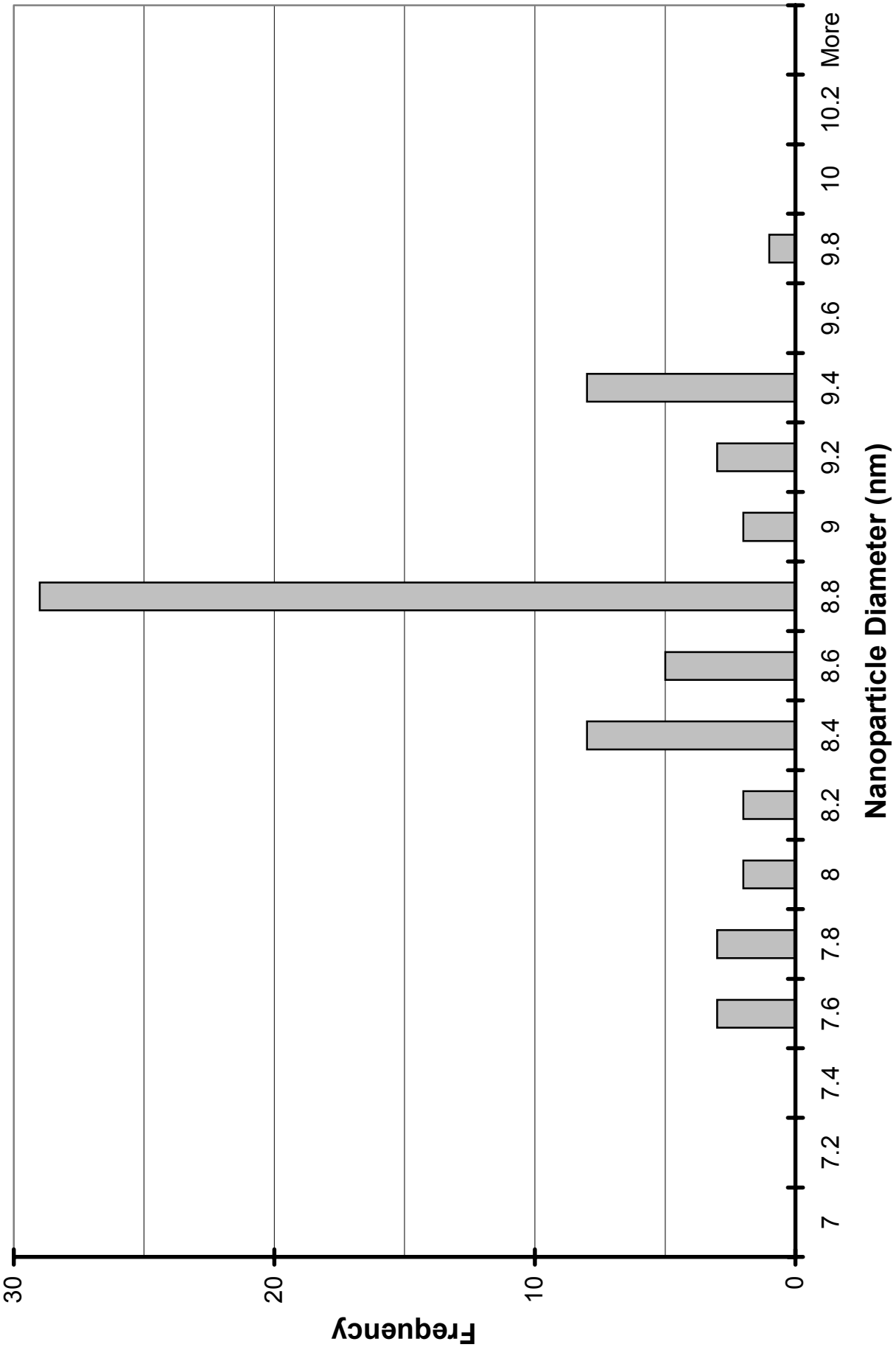

Figure 13. Particle-size histogram for sample Bi/3 (mean diameter 8.6 ± 0.5 nm)

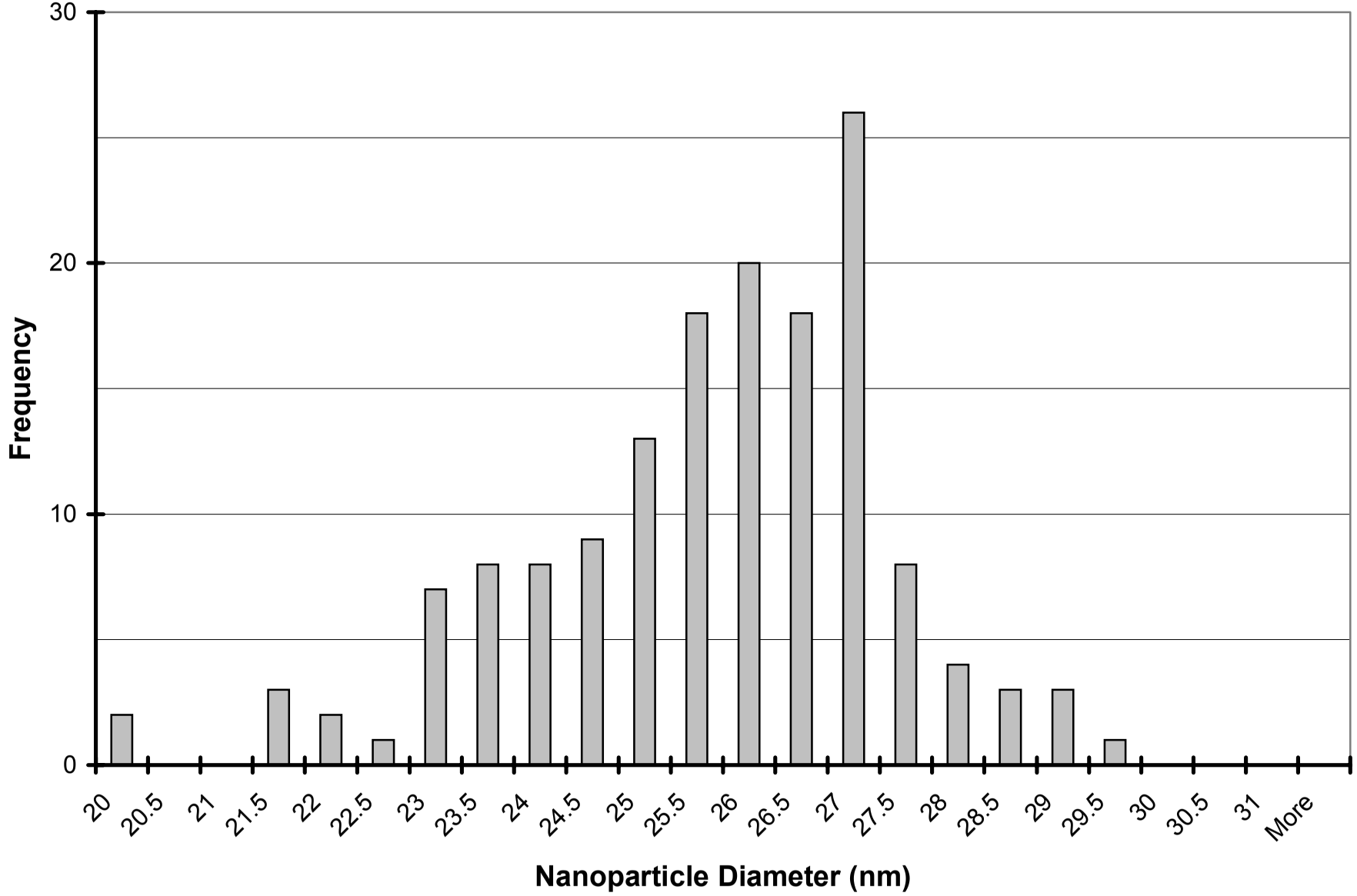

Figure 14. Particle-size histogram for sample Sn/1 (mean diameter 25.4 ± 1.8 nm)

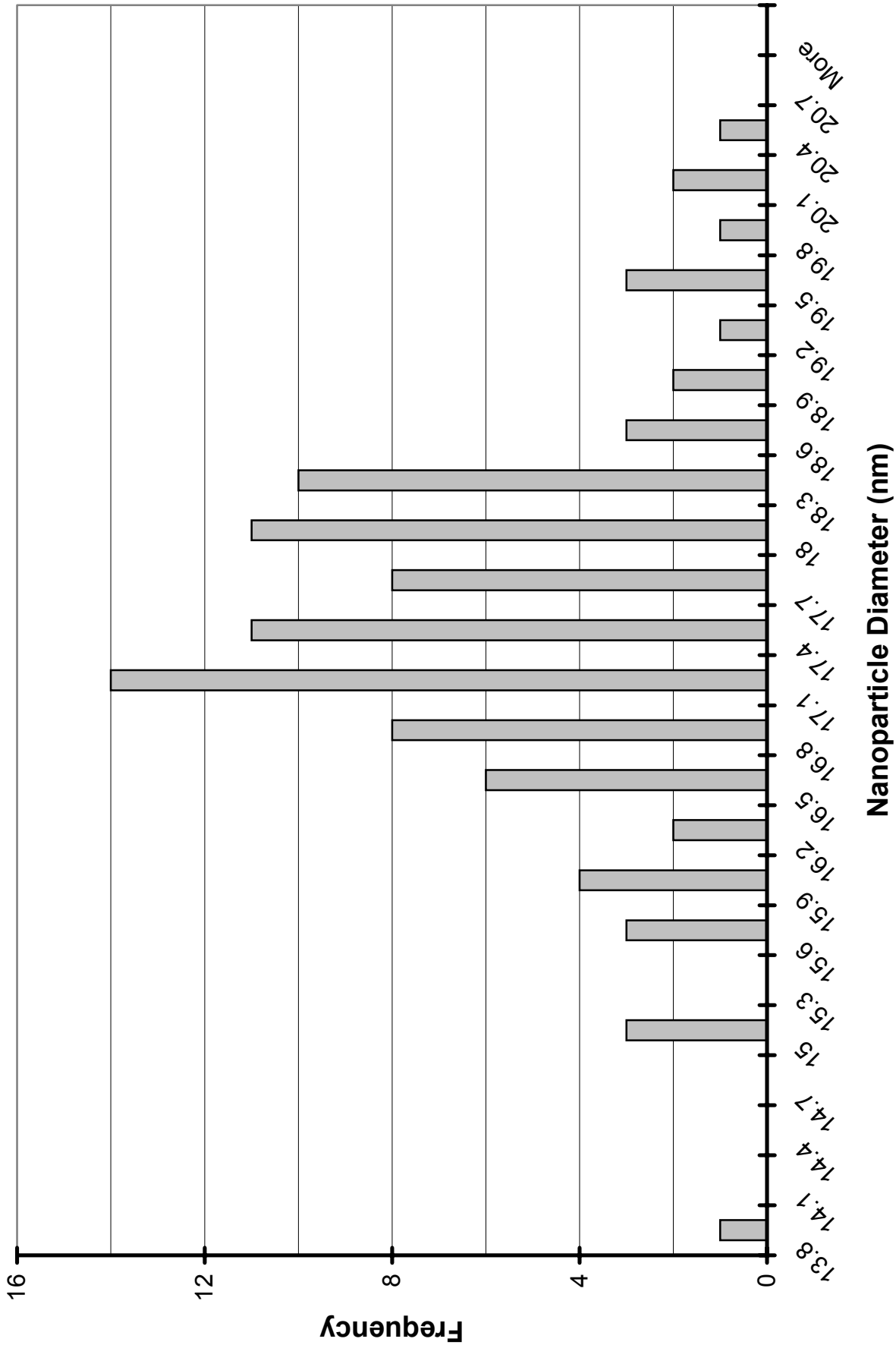

Figure 15. Particle-size histogram for sample Sn/2 (mean diameter 17.3 ± 1.2 nm)

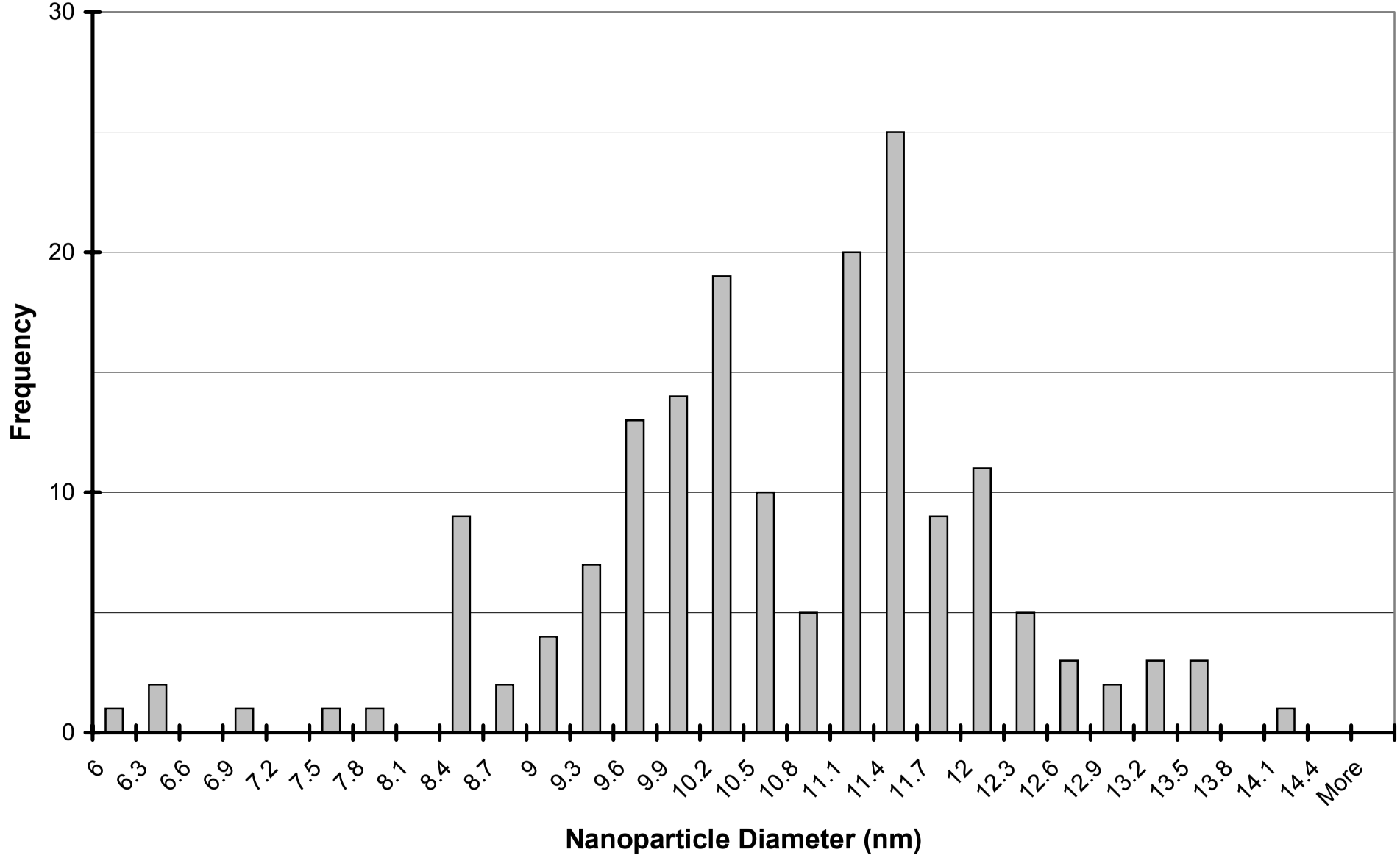

Figure 16. Particle-size histogram for sample Sn/3 (mean diameter 10.5 ± 1.4 nm)

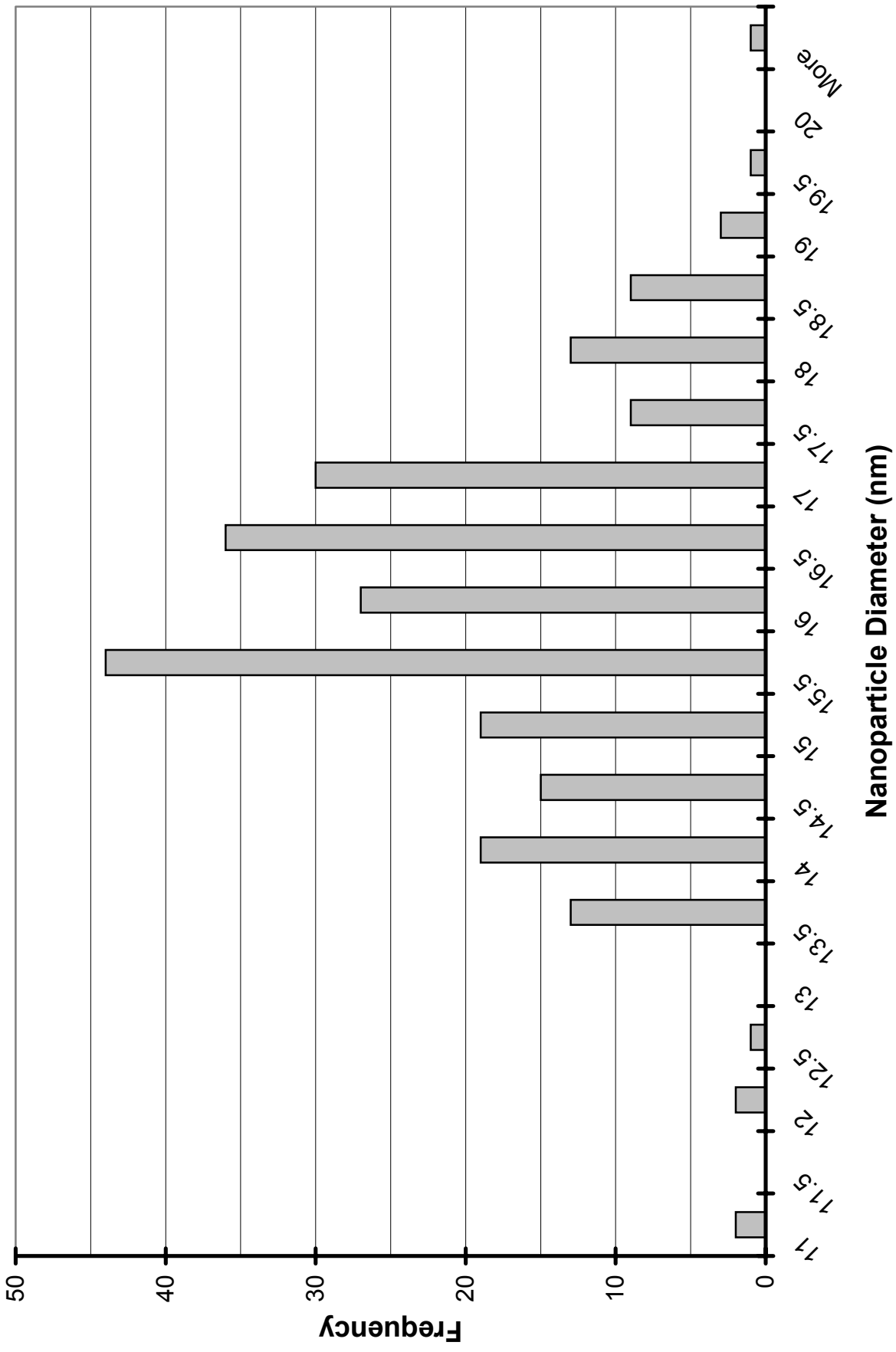

Figure 17. Particle-size histogram for sample In/1 (mean diameter 15.7 ± 1.5 nm)

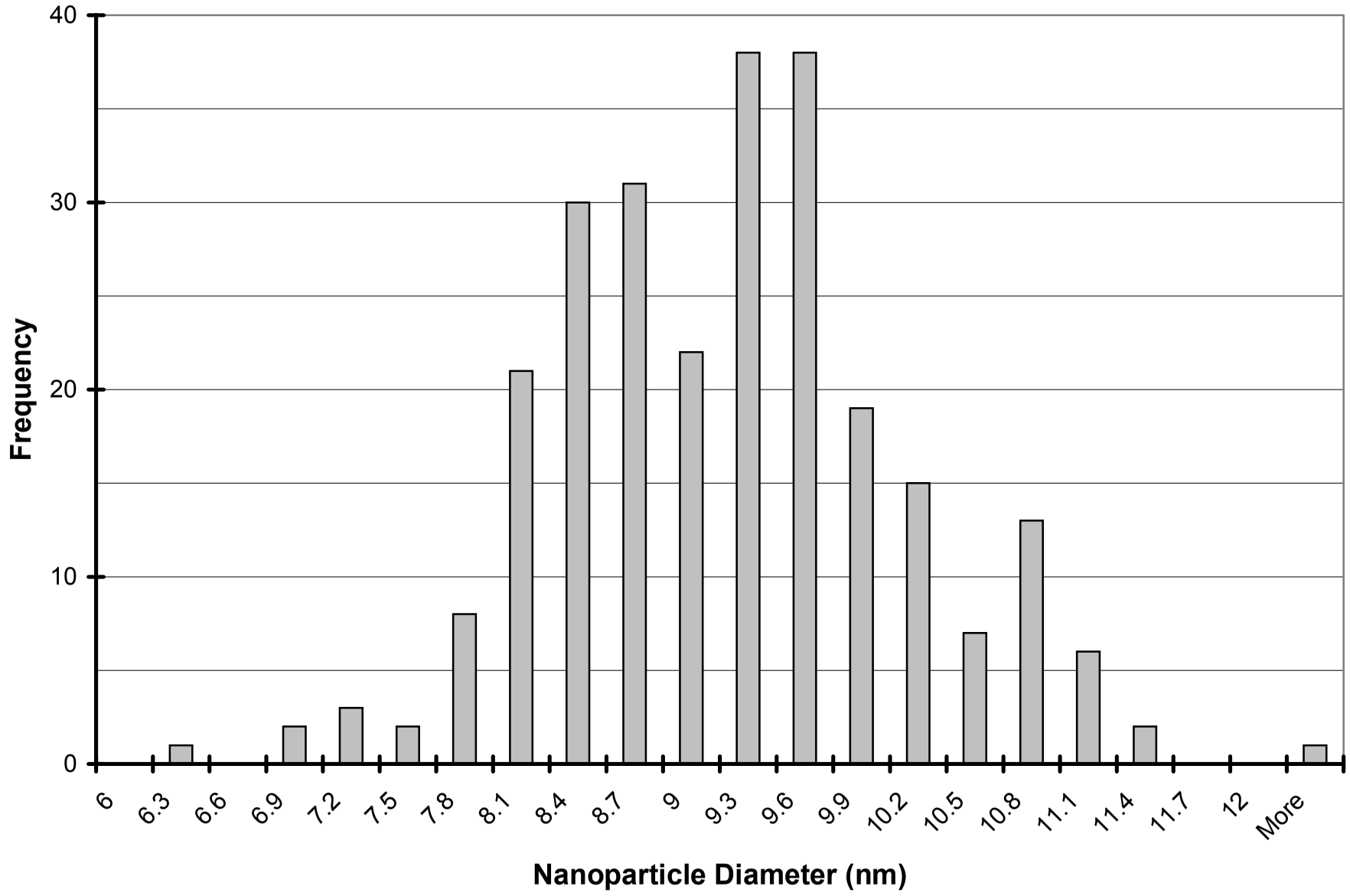

Figure 18. Particle-size histogram for sample In/2 (mean diameter 9.1 ± 0.9 nm)

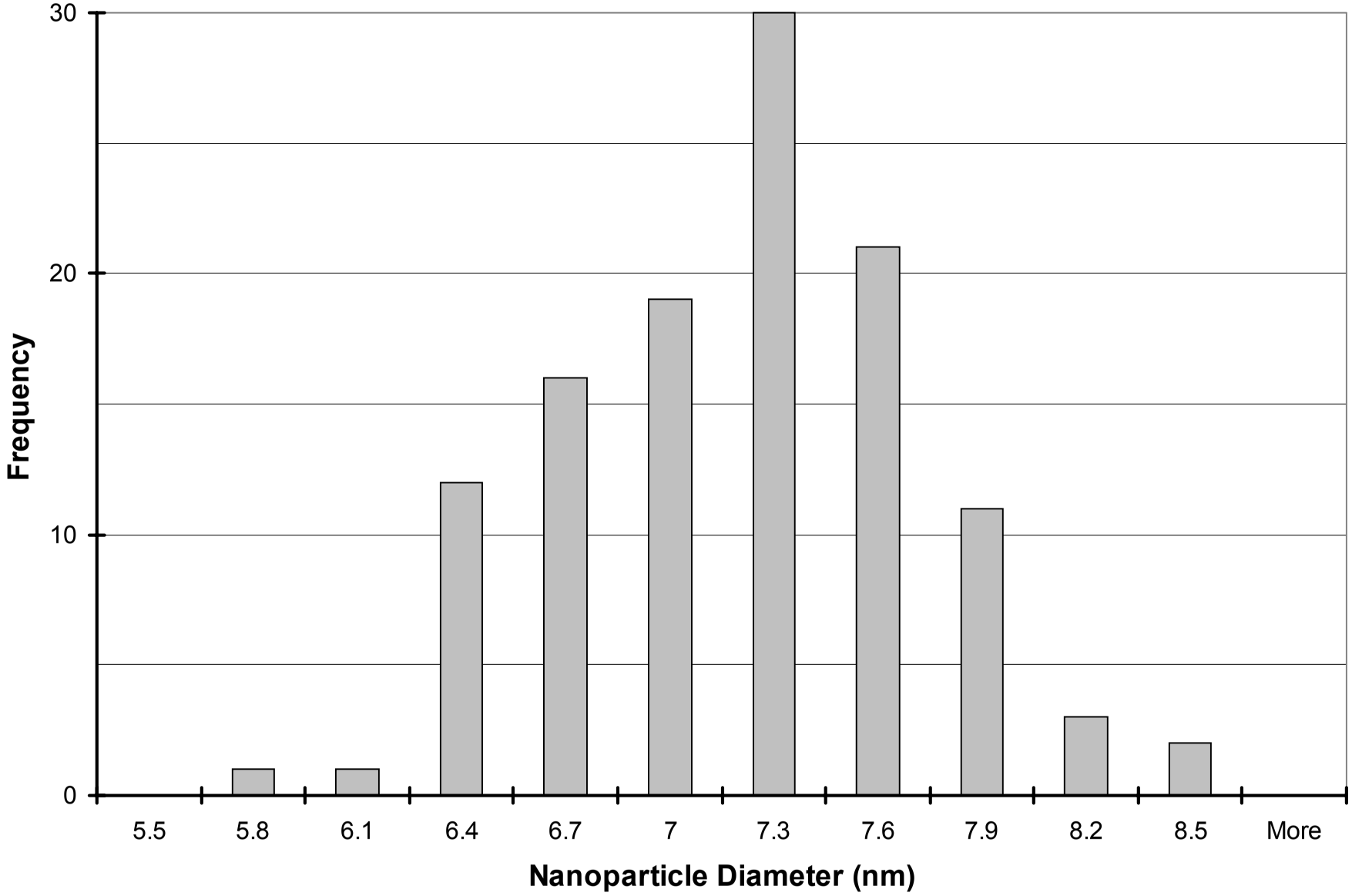

Figure 19. Particle-size histogram for sample In/3 (mean diameter 7.1 ± 0.5 nm)

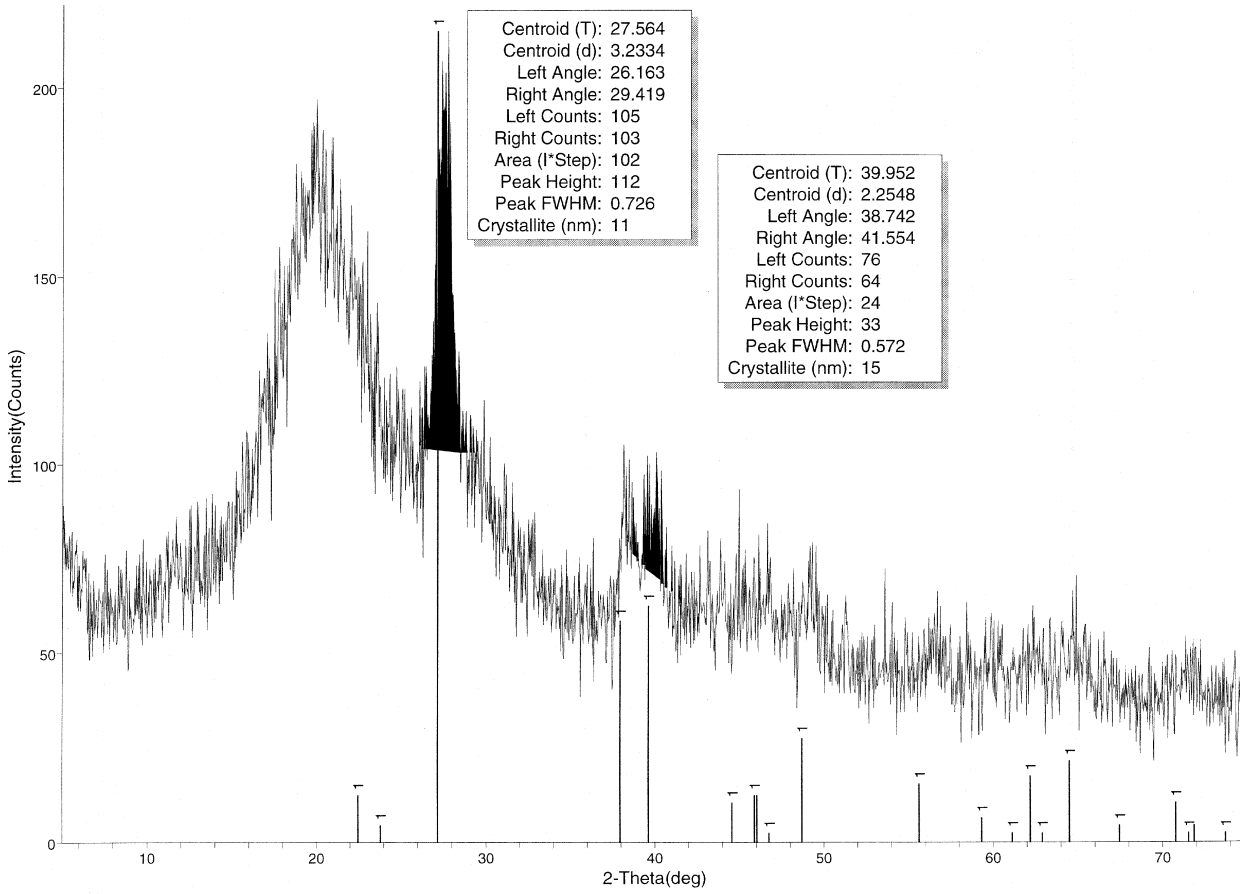

Figure 20. XRD pattern of sample Bi/1 (mean diameter 12.4 ± 0.9 nm by TEM analysis). The vertical lines labeled with a numeral "1" show the positions of the reflections in the reference pattern for crystalline Bi (JCPDS file 44-1246). The slight shifts (in 2-theta) between the observed and reference reflections result from an accidental vertical offset of the specimen in the sample holder during data collection, and do not indicate smaller lattice parameters in the sample than in the reference. The large, broad peak centered around 20 degrees 2-theta corresponds to the amorphous-polymer component of the sample. The inset boxes provide the parameters used in and produced by automated Scherrer crystalline coherence length calculations. The shaded regions are the areas used in the Scherrer calculations.

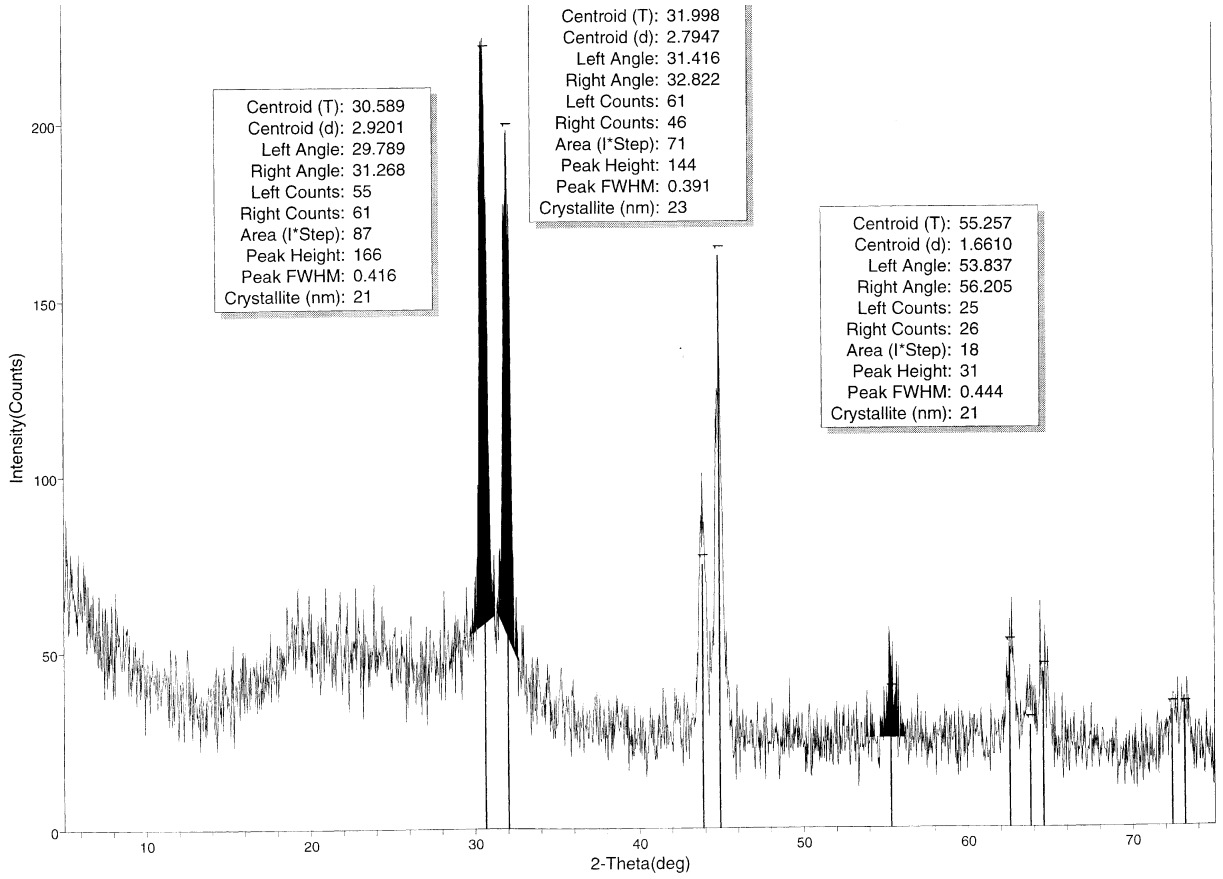

Figure 21. XRD pattern of sample Sn/1 (mean diameter 25.4 ± 1.8 nm by TEM analysis). The vertical lines labeled with a numeral "1" show the positions of the reflections in the reference pattern for crystalline Sn ($I4_1/amd$ structure, JCPDS file 04-0673). The broad peak centered around 20 – 30 degrees 2-theta corresponds to the amorphous-polymer component of the sample. The inset boxes provide the parameters used in and produced by automated Scherrer crystalline coherence length calculations. The shaded regions are the areas used in the Scherrer calculations.

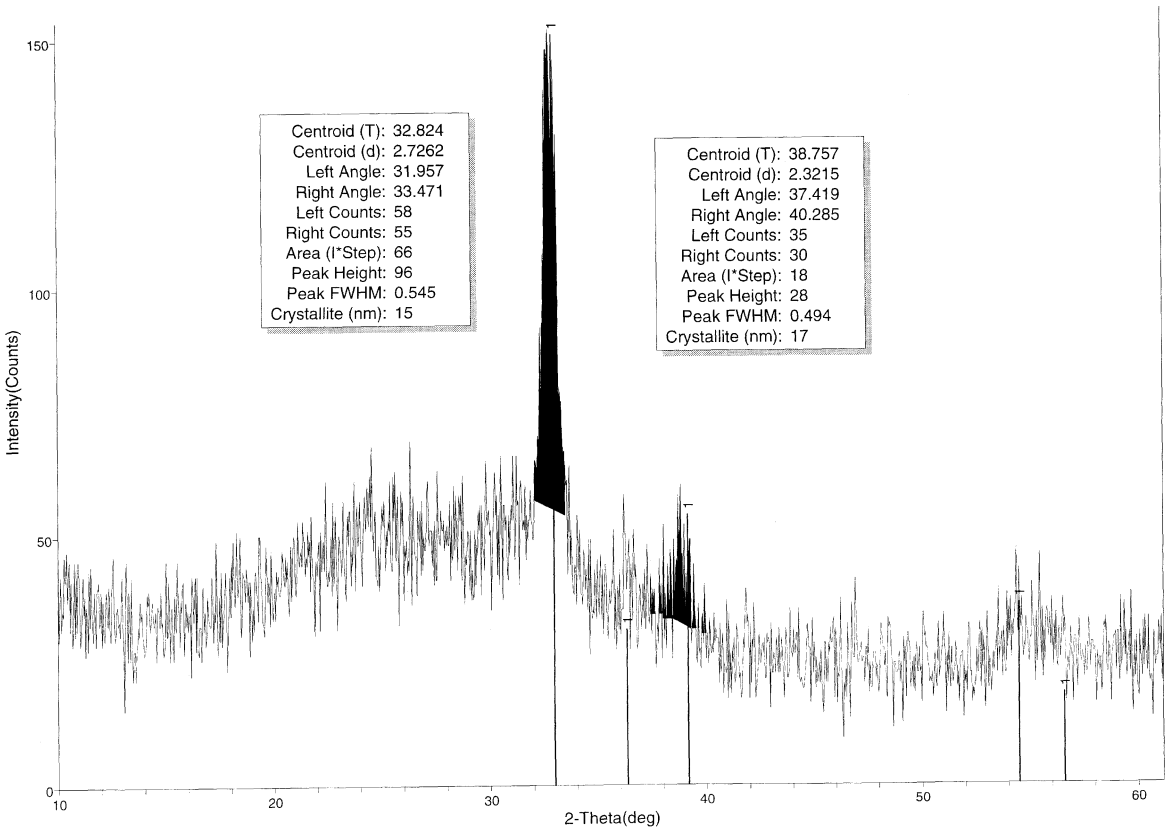

Figure 22. XRD pattern of sample In/1 (mean diameter 15.7 ± 1.5 nm by TEM analysis). The vertical lines labeled with a numeral "1" show the positions of the reflections in the reference pattern for crystalline In (JCPDS file 05-0642). The broad peak centered around 20 – 30 degrees 2-theta corresponds to the amorphous-polymer component of the sample. The inset boxes provide the parameters used in and produced by automated Scherrer crystalline coherence length calculations. The shaded regions are the areas used in the Scherrer calculations.

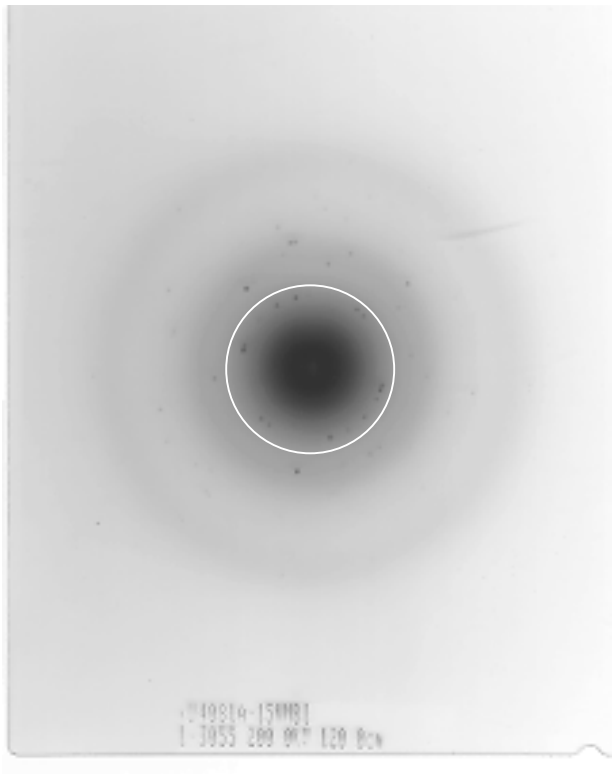

Figure 23. Electron-diffraction pattern of sample Bi/1, collected from an area containing several Bi nanoparticles. The pattern, scaled above to 100% original size, was collected at a camera length of 120.0 cm and with $\lambda_e = 0.02508$ Å. To guide the eye, a white circle is placed on the diffraction pattern at a slightly larger radius than that of the first diffraction ring (which contains several discrete, black spots). This diffraction ring indexes to the 001 reflection of Bi, and corresponds to the prominent reflection at 27 degrees 2-theta in Figure 20. From the electron-diffraction pattern, we measured a spacing $d_{001} = 3.3 \pm 0.1$ Å. For comparison, the reference Bi 001 spacing from JCPDS file 44-1246 is $d_{001} = 3.28$ Å

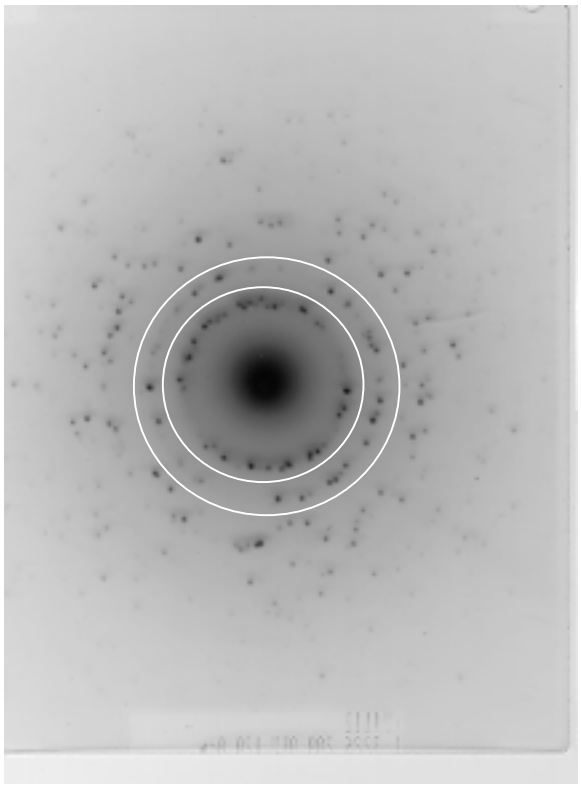

Figure 24. Electron-diffraction pattern of sample Sn/1, collected from an area containing several Sn nanoparticles. The pattern, scaled above to 100% original size, was collected at a camera length of 120.0 cm and with $\lambda_e = 0.02508$ Å. To guide the eye, white circles are placed on the diffraction pattern at slightly larger radii than those of the first two diffraction rings (which contain several discrete, black spots). *Each* of these diffraction rings corresponds to *two* closely spaced reflections. The first (smaller-radius) ring indexes to the 200/101 reflections of ($I4_1/amd$) Sn, and corresponds to the prominent reflections at 30.6 and 32.0 degrees 2-theta in Figure 21. From the electron-diffraction pattern, we measured a spacing $d_{200/101} = 2.95 – 2.74$ Å for this first (composite) diffraction ring. For comparison, the reference 200/101 Sn spacings from JCPDS file 04-0673 are $d_{200} = 2.92$ Å and $d_{101} = 2.79$ Å. The second (larger-radius) ring indicated by a white circle indexes to the 220/211 reflections of ($I4_1/amd$) Sn, and corresponds to the reflections at 43.9 and 44.9 degrees 2-theta in Figure 21. From the electron-diffraction pattern, we measured a spacing $d_{220/211} = 2.1 – 1.9$ Å for this second (composite) diffraction ring. For comparison, the reference 220/211 Sn spacings from JCPDS file 04-0673 are $d_{220} = 2.07$ Å and $d_{211} = 2.02$ Å.

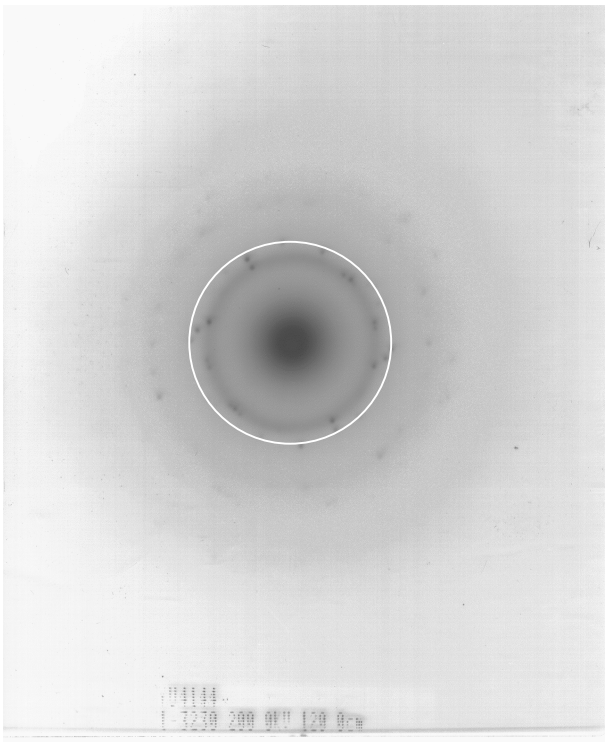

Figure 25. Electron-diffraction pattern of sample In/1, collected from an area containing several In nanoparticles. The pattern, scaled above to 100% original size, was collected at a camera length of 120.0 cm and with $\lambda_e = 0.02508$ Å. To guide the eye, a white circle is placed on the diffraction pattern at a slightly larger radius than that of the first diffraction ring (which contains several discrete, black spots). This diffraction ring indexes to the 101 reflection of In, and corresponds to the prominent reflection at 33 degrees 2-theta in Figure 22. From the electron-diffraction pattern, we measured a spacing $d_{101} = 2.7 \pm 0.1$ Å. For comparison, the reference In 101 spacing from JCPDS file 05-0642 is $d_{101} = 2.73$ Å